Coherent feedforward transcriptional regulatory motifs enhance drug resistance

Daniel A. Charlebois,[1,2,*] Gábor Balázsi,[3] and Mads Kærn[1,2,4,†]

[1]*Department of Physics, University of Ottawa, 150 Louis Pasteur, Ottawa, Ontario, Canada K1N 6N5*

[2]*Ottawa Institute of Systems Biology, University of Ottawa, 451 Smyth Road, Ottawa, Ontario, Canada K1H 8M5*

[3]*Department of Systems Biology-Unit 950, University of Texas MD Anderson Cancer Center, 7435 Fannin Street, Houston, Texas 77054, USA*

[4]*Department of Cellular and Molecular Medicine, University of Ottawa, 451 Smyth Road, Ottawa, Ontario, Canada K1H 8M5*

(Received 28 November 2013; revised manuscript received 2 February 2014; published 14 May 2014)

Fluctuations in gene expression give identical cells access to a spectrum of phenotypes that can serve as a transient, nongenetic basis for natural selection by temporarily increasing drug resistance. In this study, we demonstrate using mathematical modeling and simulation that certain gene regulatory network motifs, specifically coherent feedforward loop motifs, can facilitate the development of nongenetic resistance by increasing cell-to-cell variability and the time scale at which beneficial phenotypic states can be maintained. Our results highlight how regulatory network motifs enabling transient, nongenetic inheritance play an important role in defining reproductive fitness in adverse environments and provide a selective advantage subject to evolutionary pressure.

DOI: 10.1103/PhysRevE.89.052708 PACS number(s): 87.10.Rt, 87.16.Yc, 87.18.Tt, 87.23.Cc

I. INTRODUCTION

Gene expression is a stochastic process that enables genetically identical cells to exhibit phenotypic variation [1–4]. This noise-induced phenotypic variability can provide a fitness advantage in clonal cell populations experiencing the same drug environment [5–8]. This phenomenon may contribute to limiting the efficacy of drug therapy, including those used to treat disease caused by uncontrolled proliferation in bacterial infections [9] and cancer [10].

It was recently argued by Brock *et al.* [10] that gene expression noise may result in enduring and transiently heritable phenotypes that accelerate tumor progression by contributing to the development of drug-resistant cancer cells. In this hypothesis, phenotypic variability arising from noisy expression of a drug resistance gene allows some cells to develop a temporary insensitivity, which in turn increases the probability that a mutation conferring permanent drug immunity is acquired.

In a previous study, we investigated the effect of gene expression noise on the reproductive fitness of isogenic cell populations under stress as a first-passage time problem [11]. This study generalized and expanded previous theoretical work that explained the acute effects of drug exposure [6–8], and considered the interplay between the fluctuation amplitude and the fluctuation frequency in defining the long-term impact of gene expression noise. To analyze the problem in general terms, we used the Ornstein-Uhlenbeck process [12] to model gene expression in individual cells. This analysis revealed that the fluctuation time scale of gene expression noise is a critical parameter in determining long-term survival, and that time scales comparable to those measured in human cancer cells [13] allow for the emergence of permanent drug resistance independently of mutations [11].

Here, we investigate how the architecture of transcriptional regulatory networks can impact the development of drug resistance. This analysis is inspired by a relatively well-characterized network, the pleiotropic drug resistance (PDR) network, that provides budding yeast *Saccharomyces cerevisiae* with resistance to a broad range of drugs, and confers a drug resistance phenotype similar to that of mammalian cells by regulating the expression of ATP binding cassette (ABC) transporter genes [14]. These highly conserved genes represent the largest class of transmembrane efflux pumps responsible for multidrug resistance in microbes [15], fungi [14,16], and cancer cells [17–19]. Notably, resistance to chemotherapeutic drugs has been correlated to the expression of ABC transporter genes in tumors [18,19] and human breast cancer cells [20], and the pumps are the target of several anticancer drugs [21].

Among the 16 ABC transporter genes found in budding yeast, the pump encoded by the PDR5 gene plays several particularly important roles in cellular detoxification [22–24]. In addition to removing a broad range of structurally unrelated antibiotics from the cell, the PDR5 protein also exports toxic metabolites that accumulate during growth, and transports steroids phospholipids across the plasma membrane (see [25] for a review). PDR5 is also of particular interest with respect to fungal infections and cancers because the overexpression of drug efflux pumps belonging to the same ABC superfamily confer resistance to antibiotics in pathogenic fungi [16,26] and resistance to chemotherapy in cancerous tumors [17].

Coherent feedforward loop (FFL) motifs are ubiquitous in gene regulatory and human signaling networks [27,28] and could play important roles in the development of drug resistance. In this motif, an upstream regulatory factor activates the expression of a downstream gene directly and indirectly through a second regulator. In cases where the two regulators have redundant or partially overlapping functions, the coherent FFL naturally has a positive feedback loop (PFL) nested within it.

This combination of a coherent FFL and a PFL, hereafter denoted FFL + PFL, forms a core component of the PDR network and arises from the regulation of several ABC transporters, including the PDR5 gene, by two homologue transcription factors encoded by PDR1 and PDR3 (Fig. 1) [22], the latter of which has been shown to be autoregulated [23]. A FFL + PFL network is also known to control the expression of the ABC-transporter MDR1 that confers multidrug resistance

*daniel.charlebois@uottawa.ca

†mkaern@uottawa.ca

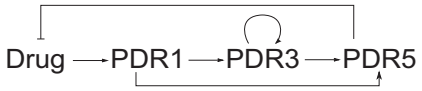

FIG. 1. Regulation of PDR5 transcription by the transcriptional regulators encoded by the PDR1 and PDR3 genes. Regular arrows denote activation and flat-head arrow denotes repression.

in human breast cancer cells [20]. However, the potential effects on the development of drug resistance of these particular network architectures have not previously been investigated.

We hypothesize that FFL motifs can facilitate the development of drug resistance by enhancing population heterogeneity in gene expression and by increasing the time scale of gene expression fluctuations to enable nongenetic inheritance. This hypothesis is based on the findings of our previous theoretical analysis [11], and previous experimental studies showing that the FFL and PFL motifs individually act to increase gene expression noise [29–31]. Moreover, it has been demonstrated experimentally that the FFL + PFL motif allows bacterial cells to prolong the maintenance of high gene expression states [32].

To examine the possible contribution of FFL motifs to the development of nongenetic drug resistance, we characterize and compare the deterministic and stochastic dynamics of individual PDR5 network components. This is done in Sec. II. Subsequently, in Sec. III, we use stochastic simulations of population dynamics to investigate how these network components impact the development of drug resistance when drug-dependent gene activation and transport of the drug across the cellular membrane is incorporated. This analysis confirms our hypothesis and demonstrates that the FFL architecture of the PDR5 transcriptional regulatory network may contribute significantly to drug resistance. Correspondingly, our study underscores that the architecture of certain gene regulatory network motifs may provide an evolutionary advantage by enhancing reproductive fitness under high-stress conditions.

II. MINIMAL MODEL

A. Modeling and simulation

The PDR5 transcriptional regulatory network in Fig. 1 can be decomposed into three elements: the direct activation (DA) of PDR5 transcription by PDR1, an FFL that combines DA with indirect activation through PDR3, and a PFL in which PDR3 activates its own expression. This decomposition defines the three distinct networks, DA, FFL, and FFL + PFL, illustrated in Fig. 2 where the three genes, PDR1, PDR3, and PDR5, are labeled X, Y, and Z, respectively.

Treating the activity of PDR1 as an adjustable, possibly time-dependent parameter x, the DA, FFL, and FFL + PFL networks have two variables whose dynamics can be described by the following system of coupled ordinary differential equations:

$$\frac{dy}{dt} = \alpha_y \omega_1 f_y(x,y) - y \tag{1}$$

$$\frac{dz}{dt} = \alpha_z f_z(x,y) - z, \tag{2}$$

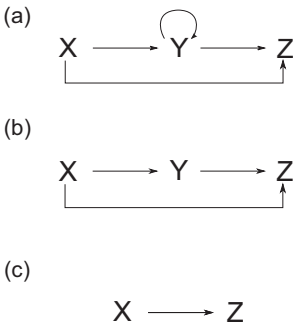

FIG. 2. PDR5 transcriptional network elements considered in the minimal model. (a) Coherent feedforward loop with positive feedback loop (FFL + PFL). (b) Coherent feedforward loop (FFL). (c) Direct activation (DA). X, Y, and Z represent respectively the PDR1, PDR3, and PDR5 genes. Arrows denote activation.

where y and z are respectively the protein concentrations associated with the expression of genes Y and Z, and α_y and α_z are the maximum level of activated protein production for Y and Z, respectively. The dilution and degradation rate of y and z are set to unity. The gene regulatory functions in Eq. (1) and Eq. (2) are defined by the Hill-type functions given by

$$f_y(x,y) = (x + \omega_2 y)^n / [K^n + (x + \omega_2 y)^n], \tag{3}$$

$$f_z(x,y) = (x + y)^n / [K^n + (x + y)^n], \tag{4}$$

where n and K are respectively the Hill coefficient and Hill constant, which for simplicity are here kept at equal values for the two genes. The activation of y by x, and the presence of positive feedback on y, are represented by the Boolean variables ω_1 and ω_2, respectively, and can be either ON ($\omega = 1$) or OFF ($\omega = 0$). Consequently, the model of the DA network is defined by $\omega_1 = \omega_2 = 0$, the FFL network by $\omega_1 = 1$ and $\omega_2 = 0$, and the FFL + PFL by $\omega_1 = 1$ and $\omega_2 = 1$. These equations were solved numerically using a medium order MATLAB intrinsic nonstiff differential equation solver (ode45).

Equations (1) and (2) can be translated into the following set of birth-death processes:

$$\varnothing \xrightarrow{k_y} y, \tag{5}$$

$$\varnothing \xrightarrow{k_z} z, \tag{6}$$

$$y \xrightarrow{\delta_y} \varnothing, \tag{7}$$

$$z \xrightarrow{\delta_z} \varnothing, \tag{8}$$

where Eq. (5) and Eq. (6) respectively describe the production of y and z. In Eq. (5), $k_y = \alpha\omega_1 f_y(x,y)$, and in Eq. (6), $k_z = \alpha f_z(x,y)$, where $f_y(x,y)$ is described in Eq. (3) and $f_z(x,y)$ in Eq. (4). The degradation of y and z are described by Eq. (7) and Eq. (8), respectively, where the degradation rates δ_y and δ_z are set to unity. Stochastic simulation of the chemical reactions were performed using the Gillespie algorithm [33].

To investigate the development of nongenetic drug resistance in clonal cell populations expressing one of these network topologies, we perform population-level simulations

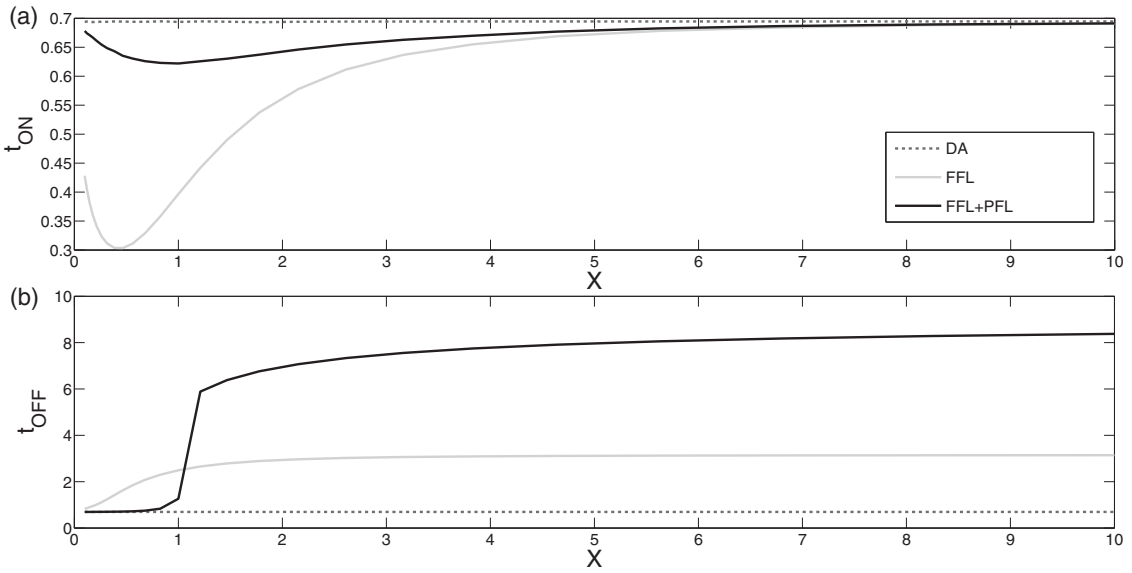

FIG. 3. Coherent feedforward networks enable fast and prolonged activation. (a) Response time t_{ON} (time for z to reach 50% of steady-state level) for the DA, FFL, and FFL + PFL networks as a function of an activating signal x. (b) Relaxation time t_{OFF} (time for z to fall to 50% of steady-state level) for the same network motifs considered in (a) as a function of x. Parameters were set to $\alpha = 10$, $n = 2$, and $K = 1$.

at single-cell resolution using the population dynamics algorithm (PDA) [34]. The PDA combines an exact method to simulate molecular-level fluctuations in single cells and a constant-number Monte Carlo approach to simulate the statistical characteristics of growing cell populations. In these simulations, gene expression in each of N individual cells is obtained by stochastically simulating Eqs. (5)–(8). Simulations were initiated by drawing the initial values of the cell cycle clock from a uniform distribution $[0,t_D]$, where t_D is the cell division time in absence of selection. Cell volume (v) was modeled using an exponential growth law,

$$v(t_{\text{div}}) = v_0 2^{t_{\text{div}}/w(z)t_D}, \tag{9}$$

where v_0 is the initial volume and t_{div} is the time since last division. At cell division, t_{div} is reset to zero, cell volume is reset to v_0, and proteins are partitioned binomially between the two daughter cells. We first model microscopic fitness (w), that is the reproductive fitness of an individual cell in the presence of a drug, using a step function. If z falls below a critical concentration (z_c) the cell is flagged and is subsequently unable to reproduce or change its protein levels. Then, we model microscopic fitness using a Hill function,

$$w(z) = z^{n_w}/\left(K_w^{n_w} + z^{n_w}\right), \tag{10}$$

where n_w and K_w are respectively the Hill coefficient and the Hill constant used to set the fitness threshold. The macroscopic fitness (W) of the population is determined by the number of cell divisions that occur during a given generation divided by the fixed number of cells in the population.

All time scales in this study are reported with respect to t_D, which is set to unit time. No qualitative difference in the results presented below was observed for up to a twofold change in parameters.

B. Results and discussion

1. *FFLs accelerate and prolong transcriptional responses*

To characterize the behavior of the DA, FFL, and FFL + PFL networks following changes in an upstream activating signal x, the response time t_{ON} and the relaxation time t_{OFF} for different values x were obtained. t_{ON} was defined as the time for z to rise from zero to 50% of the steady-state value corresponding to the DA network when x is turned ON [35,36]. t_{OFF} was similarly defined as the time, after x is turned OFF, for z to fall to 50% of the corresponding steady-state value when x is ON. The 50% DA steady-state value was chosen to ensure a controlled comparison of the three network topologies, such that the response and relaxation times for each network were determined for the same absolute change in z.

Both coherent feedforward networks decrease t_{ON} compared to the DA network [Fig. 3(a)]. There is a minimum t_{ON} at an x of about 0.5 for the FFL and FFL + PFL networks. The FFL has the quickest response time for nonzero values of x less than about 8, when the FFL and FFL + PFL t_{ON} values begin to converge. The result for FFL + PFL is particularly interesting as positive autoregulation on its own generally increases response time [37]. t_{ON} is shorter for the FFL and FFL + PFL networks for low values of x due to the presence of multiple additive activating inputs to z. The FFL + PFL network has a longer t_{ON} than the FFL network because of the positive autoregulation. For high values of x, t_{ON} for the FFL and FFL + PFL networks are similar to those of the DA network as the activation of z is dominated by the direct activation of z by x. The response time for the DA network is unaffected by varying x.

The FFL and FFL + PFL networks exhibit prolonged expression relative to the DA network [Fig. 3(b)]. These results are in qualitative agreement with previous theoretical predictions [38] and experimental results [32]. Notably, the FFL + PFL network has the longest t_{OFF} for x values larger than 1, and the FFL network has the longest t_{OFF} for nonzero x

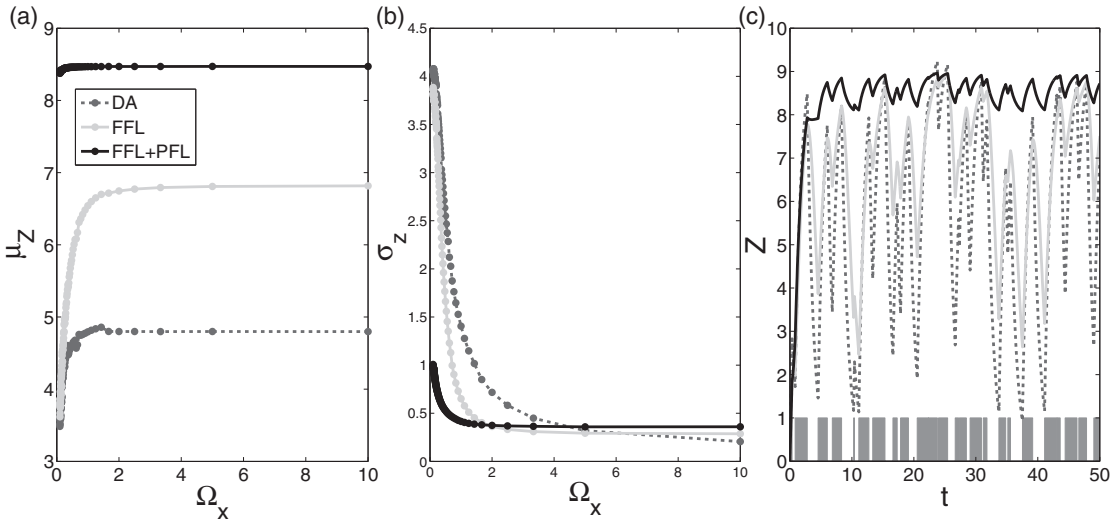

FIG. 4. Response of z to a fluctuating upstream activating signal. (a) The mean of z (μ_z) is shown for the DA, FFL, and FFL + PFL networks as a function of the ON-OFF switching frequency of x (Ω_x). (b) The standard deviation of z (σ_z) is shown for the same network motifs considered in (a) as a function of Ω_x. (c) z as a function of a randomly fluctuating Ω_x (dark gray rectangles denote the presence of an activating signal) for the same network motifs considered in (a). Parameters were set to $x_{ON} = 5$, $x_{OFF} = 0$, $\alpha = 10$, $n = 2$, and $K = 1$.

values less than 1. The relatively long t_{OFF} of the FFL + PFL network can be attributed to the PFL which has been shown to increase relaxation time [35,36]. The threshold occurs at 1 as K (which specifies the input value at which half-maximal protein production occurs in the output) rate was set to unity. When x is increased above K, the positive feedback on y is activated and the response time increases. The t_{OFF} for the DA network is unaffected by changing x values [Fig. 3(b)].

When considering the t_{ON} and t_{OFF} together for x values less than 1, the FFL has both a larger t_{ON} and t_{OFF} compared to the FFL + PFL and DA networks (Fig. 3). When x is increased by an order of magnitude, though the three networks have similar t_{ON} values, the FFL + PFL network has a larger t_{OFF}. These results suggest that if z confers drug resistance, the FFL network provides a fitness advantage when the activating signal (i.e., the drug dose) is low, and the FFL + PFL network a fitness advantage when the drug dose is high.

2. FFLs provide stable high expression in fluctuating environments

To investigate how the three networks respond to a fluctuating upstream activating signal, x was set to switch between ON and OFF at a frequency Ω_x. The value of x was set to 5 when it was ON and zero when it was OFF.

When x fluctuates periodically, the mean concentration of z (μ_z) is higher in the FFL + PFL network compared to the other two networks [Fig. 4(a)], despite all three networks having the same mean when x is held constant (data not shown). μ_z is higher in the FFL network than the DA network, with both networks increasing μ_z with increasing values of Ω_x until they level off at around $\Omega_x = 2$. The higher μ_z in the FFL and FFL + PFL networks occurs because coherent feedforward networks buffer against input fluctuations [39].

The frequency-response plot for the three networks shows that the standard deviation of z (σ_z) in the FFL and FFL + PFL is lower than σ_z for the DA when Ω_x is less than about 4.5 [Fig. 4(b)]. As Ω_x is increased above 4.5, σ_z for the DA network falls below the σ_z values for the FFL and the FFL + PFL networks. The FFL + PFL network has lower values of σ_z than the FFL network until Ω_x is increased to about 2; then the σ_z value for the FFL falls below that of the FFL + PFL for higher values of Ω_x.

When x is set to fluctuate randomly, the FFL + PFL network provides stable high expression compared to the FFL and DA networks [Fig. 4(c)].

3. FFLs increase population heterogeneity and mixing times

The set of chemical reactions [Eqs. (5)–(8)] corresponding to the deterministic model [Eqs. (1) and (2)] were simulated stochastically to compare the noise and mixing times of the three networks. The mixing time was defined previously by Sigal *et al.* [13] as the time for the autocorrelation function to decay by half.

The noise in network output z ($\eta_z = \sigma_z/\mu_z$) for the three network motifs was compared at the same μ_z [Fig. 5(a)]. For a given μ_z, $\eta_z = \sigma_z/\mu_z$ is the highest for the FFL + PFL network. The increase in noise due to positive feedback is expected as it amplifies fluctuations [40]. η_z for the DA and FFL are similar, with η_z for all three networks beginning to converge for μ_z around 5.

As x is varied, the relaxation times are highest for the FFL + PFL network, followed by the FFL network and then the DA network [Fig. 5(b)]. The longer relaxation time in the FFL + PFL network compared to the DA network is qualitatively in agreement with results found experimentally by Kalir *et al.* [32].

4. FFLs enhance drug resistance

Gene expression [Eqs. (5)–(8)] was coupled to population dynamics using the PDA [34] to investigate the effects of feedforward network motifs on drug resistance.

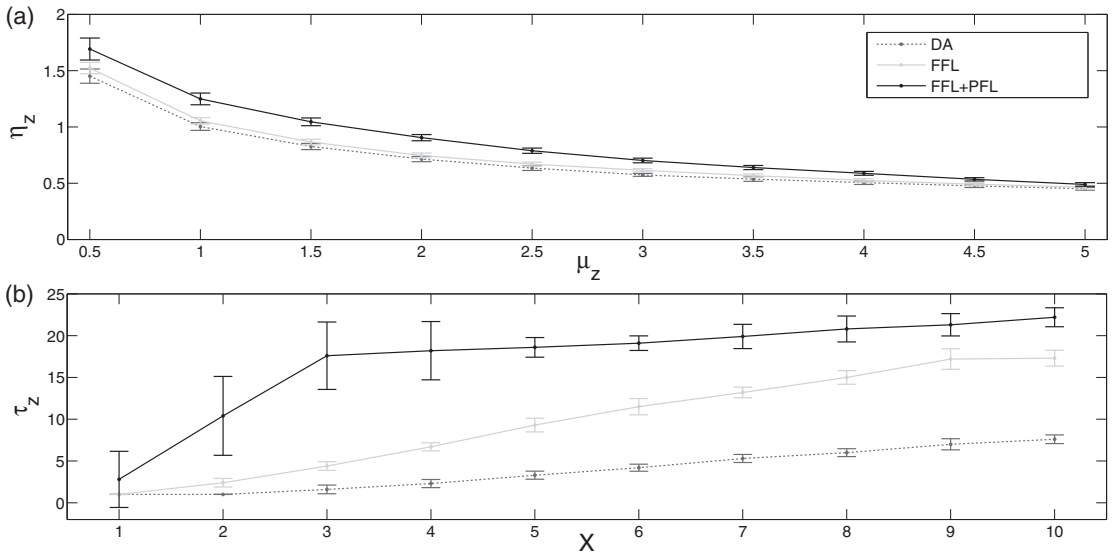

FIG. 5. Coherent feedforward networks increase noise and relaxation time. (a) The noise in z (η_z) for the DA, FFL, and FFL + PFL networks as a function of the mean level of z (μ_z). (b) The response times for z (τ_z) for the same network motifs considered in (a) as a function of an activating signal x. Parameters were set to $\alpha = 10$, $n = 2$, and $K = 10$. Ten realizations for 10^3 arbitrary time units were performed. Error bars show standard deviation.

Prior to the application of the drug at generation 10 the fitness is 1, as all the cells in the population divide once per generation (Fig. 6). When we consider a threshold fitness function, all the cells in DA population are unable to reproduce immediately following application of the drug [Fig. 6(a)]. A significant fraction of cells in the FFL and FFL + PFL populations remain fit even after 40 generations of drug treatment.

Next we model microscopic fitness using Eq. (10). Interestingly, in this model, drug resistance develops in all three populations [Fig. 6(b)]. A much lower number of cells in the generation subsequent to the application of the drug reproduce as a result of low z level due to the transient time of z to the new steady state. After a couple of oscillations, the fitness levels off such that a fraction of the pretreatment population reproduces in each generation. The fraction of fit cells during drug treatment is roughly double for the FFL and FFL + PFL populations compared to the DA population.

These results, together with the results from Secs. II B 1–II B 3, suggest that in natural populations the coherent

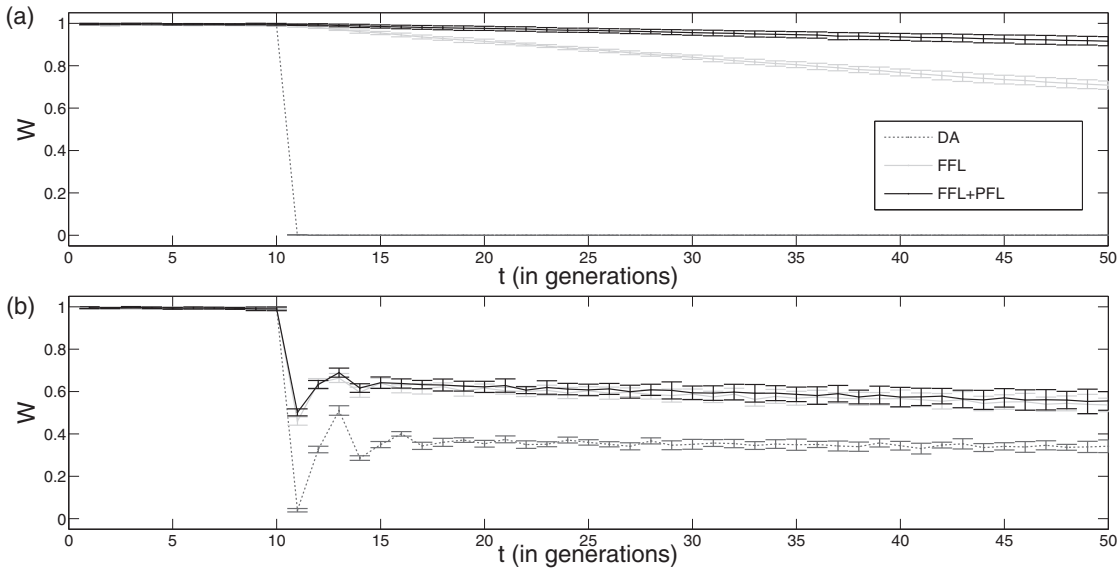

FIG. 6. Effect of network topology and fitness threshold on reproductive fitness (W). W for each of the DA, FFL, and FFL + PFL populations over 50 generations. Drug treatment is initiated at the tenth generation. (a) Population simulations using a step fitness function. (b) Population simulations performed using a Hill type fitness function. Parameters were set to $x = 1$, $\alpha_y = 10$, $\alpha_z = 100$, $K = 1$, and $n = 2$. In (a) $z_c = 35$ and in (b) $K_w = 35$, and $n_w = 2$. Ten realizations of 1000 cells were performed. Error bars show standard deviation.

feedforward network architecture may provide cells with a fitness advantage in adverse environments due to increased noise, faster response, and longer relaxation times. The PFL enhances all of these properties except the response time. Interestingly, the FFL + PFL network forms the topology of a network which regulates the expression of the PDR5 and MDR1 multidrug resistance conferring proteins in yeast [14] and breast cancer cells [20]. It is plausible that the FFL + PFL architecture, investigated in the next section in the context of the PDR5 transcriptional network, evolved by means of natural selection due to the fitness advantage it provides in the drug environment.

III. PDR5 TRANSCRIPTIONAL NETWORK MODEL

A. Modeling and simulation

In this section, we develop a mathematical model and simulate the dynamics of the PDR5 transcriptional regulatory network in order to investigate the development of drug resistance in the context of a more biologically realistic feedforward genetic network, incorporating passive and active diffusion of a drug across the cellular membrane. This section presents a model of the PDR5 transcription network.

To examine if the conclusions from the analysis of minimal network models have bearing on PDR5-mediated drug resistance, we analyzed a model of the regulatory network in Fig. 1. This network differs from the FFL + PFL network in Sec. II by the presence of a negative feedback loop caused by the PDR5 efflux pump eliminating drugs and toxins from the cell. We note that the additivity of the gene regulatory functions in the minimal model [Eqs. (1) and (2)] are justified in the context of PDR5 transcriptional regulation because PDR1 and PDR3 are highly homologous and bind to the same elements in the PDR5 promoter [22]. Consequently, the PDR5 network can be modeled by extending the minimal model to include the upstream activating factor (PDR1) and the intracellular drug (D_{int}) as dynamic variables. The resulting ordinary differential equations (note that in the equations below PDR1, PDR3, and PDR5 are represented by x, y, and z, respectively) describing the network are given by

$$\frac{dx}{dt} = \alpha_0 + \alpha_1 \frac{D_{\text{int}}}{K_1 + D_{\text{int}}} - \delta_1 x, \tag{11}$$

$$\frac{dy}{dt} = \alpha_3 \frac{(x+y)^{n_3}}{\left[K_3^{n_3} + (x+y)^{n_3}\right]} - \delta_3 y, \tag{12}$$

$$\frac{dz}{dt} = \alpha_5 \frac{(x+y)^{n_5}}{\left[K_5^{n_5} + (x+y)^{n_5}\right]} - \delta_5 z, \tag{13}$$

$$\frac{d(D_{\text{int}})}{dt} = k_{\text{diff}}(D_{\text{ext}} - D_{\text{int}}) - \frac{k_{\text{pump}} z D_{\text{int}}}{k_{\text{pump}} + D_{\text{int}}}, \tag{14}$$

when it is assumed that the drug enters and leaves the cell through a combination of passive and active transport, and that the activation of PDR1 by the drug can be captured by Michaelis-Menten kinetics. Equation (11) describes the activation of PDR1 by D_{int}, where α_0 is the basal rate of transcription and $\alpha_0 + \alpha_1$ the maximal activated rate of transcription. Equations (12) and (13) are the same as those presented in Eqs. (1) and (2). The last equation, Eq. (14), describes the passive diffusion of the drug across the cell membrane [first term on the right-hand side (RHS)], as well as the pumping of the drug out of the cell via PDR5 (second term on the RHS). In Eq. (14), D_{ext} is the extracellular drug concentration, k_{diff} the rate of passive diffusion across the cell membrane, and k_{pump} the rate of PDR5 mediated drug efflux.

The PDR network model [Eqs. (11)–(14)] can be translated into the corresponding birth-death processes:

$$\oslash \xrightarrow{k_1} x, \tag{15}$$

$$\oslash \xrightarrow{k_3} y, \tag{16}$$

$$\oslash \xrightarrow{k_5} z, \tag{17}$$

$$x \xrightarrow{\delta_1} \oslash, \tag{18}$$

$$y \xrightarrow{\delta_3} \oslash, \tag{19}$$

$$z \xrightarrow{\delta_5} \oslash, \tag{20}$$

$$\oslash \xrightarrow{k_{D_{\text{int}}}} D_{\text{int}}, \tag{21}$$

$$D_{\text{int}} \xrightarrow{\delta_{D_{\text{int}}}} \oslash, \tag{22}$$

where $k_1 = \alpha_0 + \alpha_1 D_{\text{int}}^{n_1}/(K_1^{n_1} + D_{\text{int}}^{n_1})$, $k_3 = \alpha_3(x+y)^{n_3}/[K_3^{n_3} + (x+y)^{n_3}]$, $k_5 = \alpha_5(x+y)^{n_5}/[K_5^{n_5} + (x+y)^{n_5}]$, $k_{D_{\text{int}}} = k_{\text{diff}} D_{\text{ext}}$, and $\delta_{D_{\text{int}}} = k_{\text{diff}} + k_{\text{pump}} z/(k_{\text{pump}} + D_{\text{int}})$. Equations (15)–(17) respectively describe the production of PDR1, PDR3, and PDR5. The degradation of PDR1, PDR3, and PDR5 is described by Eqs. (18)–(20), respectively. The passive diffusion of the drug into the cell is described by Eq. (21). The removal of the drug from the cell by both passive diffusion and pumping is described by Eq. (22). Here we model cell growth using Eq. (9) and cellular fitness in the presence of a drug as follows:

$$w(z) = z/(D_{\text{int}} + z). \tag{23}$$

This equation describes cellular fitness increasing with increasing PDR5 relative to the intracellular drug concentration, and it assumes that there is no fitness cost associated with maintaining a high level of PDR5.

B. Results and discussion

In order to investigate if persistent nongenetic drug resistance would develop in the PDR5 transcriptional network model, we tracked cellular and fitness dynamics over 50 generations.

In Fig. 7(a), the population PDR5 histogram prior to drug treatment is shown (generation 9) together with the population PDR5 histogram after 40 generations of drug treatment (generation 50). The corresponding mean PDR5 expression increases threefold upon application of the drug,

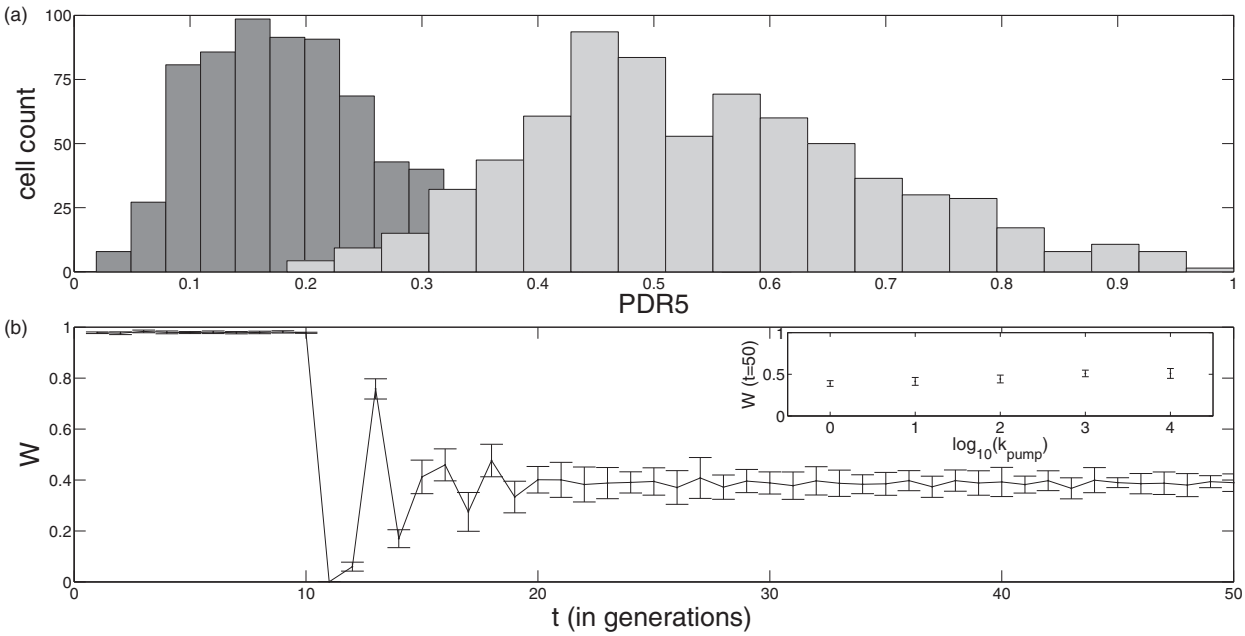

FIG. 7. Adaptation and fitness (W) facilitated by the PDR5 transcriptional network. (a) Number of cells in the population has the corresponding PDR5 expression level. Distributions are shown for the generation prior (dark gray) to drug application and 40 generations after (light gray) drug application. (b) W over 50 generations. Inset shows W at generation 50 for different rates of PDR5 mediated drug efflux (k_{pump}). Drug treatment is initiated at the tenth generation. Unless otherwise indicated, parameters were set to $\alpha_0 = 1$, $\alpha_1 = 10$, $K_1 = 1$, $n_1 = 1$, $\alpha_3 = 10$, $K_3 = 1$, $n_3 = 2$, $\alpha_5 = 100$, $K_5 = 20$, $n_5 = 2$, $k_{\text{diff}} = 100$, $k_{\text{pump}} = 1$, and $D_{\text{ext}} = 100$. Ten realizations of 1000 cells were performed.

in agreement with preliminary experimental data obtained in our laboratory for budding yeast populations after 24 h of drug (Nocodazole) treatment (data not shown).

The resulting drug resistance dynamics in Fig. 7(b) are similar to those obtained using the minimal model with a Hill type fitness function [Fig. 6(b)]. Namely, a stable fraction of reproductively viable cells develops after about 10 generations of drug treatment. When the rate of passive diffusion (k_{diff}) and extracellular drug concentration (D_{ext}) are changed the level of fitness changes accordingly. For instance, when k_{diff} and D_{ext} are decreased 10 fold, the steady-state W increases to 0.9 (data not shown).

The main difference between the minimal model and the PDR5 model is the incorporation of negative feedback on the activating signal in the latter. In order to investigate the effects of the negative feedback on fitness, we varied k_{pump} over several orders of magnitude [inset Fig. 7(b)]. Fitness after 40 generations of drug treatment increased from 0.39 when $k_{\text{pump}} = 1$ to 0.51 when $k_{\text{pump}} = 10^4$. As expected, when $k_{\text{pump}} = 0$, W is zero for all generations subsequent to drug application (data not shown).

These results demonstrate that the presence of a negative feedback in a drug-efflux pump network does not impede the development of persistent nongenetic drug resistance. Increasing the strength of the negative feedback had little effect on the fraction of drug resistant cells in the population. This is because although PDR5 functions to increase cellular fitness by actively pumping the drug out of the cell, it also reduces its own activation by indirectly reducing the activity of PDR1.

IV. CONCLUSION

This study demonstrates that certain transcriptional regulatory network motifs can facilitate the development of drug resistance by providing a broader spectrum of potentially advantageous fitness phenotypes upon which selection can act, and by enabling the inheritance of these transient phenotypes to subsequent generations. While it is well established that genetic mutations can cause drug tolerance [41–45], much less is known about how gene expression noise can influence drug resistance. Correspondingly, the findings in our study make an important contribution to a growing body of research establishing that drug resistance can result from phenotypic heterogeneity in clonal cell populations [9,11,46,47].

Previous work on the role of noise in drug resistance has investigated the possible effects of stochastic switching between distinct phenotypic states (e.g., [46,48,49]). Such switching may be linked to bistability in an underlying gene regulatory network with state transitions driven by gene expression noise. Bistability may arise from positive feedback loops, and has, for example, been demonstrated experimentally to enable robust inheritance of gene expression states [50]. However, while bistability provides a mechanism for nongenetic inheritance in nonresponsive adaptation, it is not a prerequisite for the development of permanent drug resistance.

The development of drug resistance through nonresponsive adaptation requires that beneficial gene expression levels be maintained over subsequent generations [6,8,11]. For example, it was recently proposed that the selection of lineages characterized by infrequent pulses of gene expression could allow nonresponsive adaptation during prolonged drug exposure [9],

and the authors proposed several hypothetical scenarios that might facilitate lineage selection without bistability. We have demonstrated previously that the minimum time scale for noise-induced drug resistance is on the order of the cell cycle [11].

In the present work, we have focused on investigating how transcriptional regulatory motifs may impact the development of drug resistance in a system, the pleiotropic drug resistance network, that is known to reduce the sensitivity of budding yeast to a broad range of structurally and functionally unrelated drugs [22]. Although the presence of a coherent feedforward loop and positive feedback loop in this network has been known for some time, it has not previously been demonstrated that this particular network architecture may be highly beneficial during prolonged drug exposure even in the case of responsive adaptation. A similar coherent feedforward network has also been proposed to be critical in the context of drug resistance of human cancer cells [20]. In addition to feedforward networks, other motifs may facilitate the development of drug resistance such as those that regulate bursty gene expression [11].

Our study demonstrates that the coherent feedforward network impacts the development of drug resistance by prolonging the time that beneficial gene expression states can be maintained. This potential mechanism for transient nongenetic inheritance has been demonstrated experimentally in *E. coli* [32]. Positive feedback regulation can further amplify this effect even without enabling an underlying bistability. However, positive feedback regulation is not necessary for the development of permanent drug immunity as the feedforward motif can provide the required nongenetic inheritance on its own. The selective advantage provided by coherent feedforward networks in the context of reduced sensitivity to toxic compound exposure may have contributed to the prevalence of this motif in present day organisms.

ACKNOWLEDGMENTS

The authors would like to thank Afnan Azizi and Ian Roney for helpful discussions. D.C. was supported financially by a Queen Elizabeth II Graduate Scholarship in Science and Technology from the Government of Ontario and an Excellence Scholarship from the University of Ottawa. G.B. was supported by the NIH Director's New Innovator Award Program (Grant No. 1DP2 OD006481-01).

[1] A. Eldar and M. B. Elowitz, Nature (London) **467**, 167 (2010).
[2] M. B. Elowitz, A. J. Levine, E. D. Siggia, and P. S. Swain, Science **297**, 1183 (2002).
[3] M. Kaern, T. C. Elston, W. J. Blake, and J. J. Collins, Nat. Rev. Genet. **6**, 451 (2005).
[4] B. B. Kaufmann and A. van Oudenaarden, Curr. Opin. Genet. Dev. **17**, 107 (2007).
[5] W. J. Blake, G. Balazsi, M. A. Kohanski, F. J. Issacs *et al.*, Mol. Cell **24**, 853 (2006).
[6] D. Fraser and M. Kaern, Mol. Microbiol. **71**, 1333 (2009).
[7] L. J. Zhang, S. W. Yan, and Y. Z. Zhuo, Acta Phys. Sin. **56**, 2442 (2007).
[8] D. Zhuravel, D. Fraser, S. St-Pierre, L. Tepliakova *et al.*, Syst. Synth. Biol. **4**, 105 (2010).
[9] Y. Wakamoto, N. Dhar, R. Chait, K. Schneider *et al.*, Science **339**, 91 (2013).
[10] A. Brock, H. Chang, and S. Huang, Nat. Rev. Genet. **10**, 336 (2009).
[11] D. A. Charlebois, N. Abdennur, and M. Kaern, Phys. Rev. Lett. **107**, 218101 (2011).
[12] G. E. Uhlenbeck and L. S. Ornstein, Phys. Rev. **36**, 823 (1930).
[13] A. Sigal, R. Milo, A. Cohen, N. Geva-Zatorsky *et al.*, Nature (London) **444**, 643 (2008).
[14] M. Kolaczkowski, A. Kolaczowska, J. Luczynski, S. Witek, and A. Goffeau, Microb. Drug. Resist. **4**, 143 (1998).
[15] J. Lubelski, W. N. Konings, and A. J. M. Driessen, Microbiol. Mol. Biol. Rev. **71**, 463 (2007).
[16] D. Sanglard and F. C. Odds, Lancet Infect. Dis. **2**, 73 (2002).
[17] B. E. Bauer, K. Kuchler, and H. Wolfger, Biochim. Biophys. Acta **1461**, 217 (1999).
[18] A. Persidis, Nat. Biotechnol. **17**, 94 (1999).
[19] K. W. Scotto, Oncogene **22**, 7496 (2003).
[20] S. Misra, S. Ghatak, and B. Toole, J. Biol. Chem. **280**, 20310 (2005).
[21] G. D. Leonard, O. Polgar, and S. E. Bates, Curr. Opin. Investig. Drugs **3**, 1652 (2002).
[22] E. Balzi and A. Goffeau, J. Bioenerg. Biomembr. **27**, 71 (1995).
[23] A. Delahodde, T. Delaveau, and C. Jacq, Mol. Cell. Biol. **15**, 4043 (1995).
[24] K. Gulshan and W. Scott Moye-Rowley, Eukaryot. Cell. **6**, 1933 (2007).
[25] R. Prasad and A. Goffeau, Annu. Rev. Microbiol. **66**, 39 (2012).
[26] K. Izumikawa, H. Kakeya, H. F. Tsai, B. Grimberg *et al.*, Yeast **20**, 249 (2003).
[27] D.-H. Le and Y.-K. Kwon, Bioinf. **29**, 630 (2013).
[28] R. Milo, S. Shen-Orr, S. Itzkovitz, N. Kashtan *et al.*, Science **298**, 824 (2002).
[29] M. Acar, A. Becskei, and A. van Oudenaarden, Nature (London) **435**, 228 (2005).
[30] D. Orrell and H. Bolouri, J. Theor. Biol. **230**, 301 (2004).
[31] V. Shahrezaei, J. F. Ollivier, and P. Swain, Mol. Syst. Biol. **4**, 196 (2008).
[32] S. Kalir, S. Mangan, and U. Alon, Mol. Syst. Biol. **1**, 2005.0006 (2005).
[33] D. T. Gillespie, J. Phys. Chem. **81**, 2340 (1977).
[34] D. A. Charlebois, J. Intosalmi, D. Fraser, and M. Kaern, Commun. Comput. Phys. **9**, 89 (2011).
[35] M. A. Savageau, Nature (London) **252**, 546 (1974).
[36] N. Rosenfeld, M. B. Elowitz, and U. Alon, J. Mol. Biol. **323**, 785 (2002).
[37] U. Alon, *An Introduction to Systems Biology: Design Principles of Biological Circuits* (Chapman & Hall/CRC, Boca Raton, 2007).
[38] S. Mangan and U. Alon, Proc. Natl. Acad. Sci. USA **100**, 11980 (2003).
[39] S. Shen-Orr, R. Milo, S. Mangan, and U. Alon, Nat. Genet. **31**, 64 (2002).
[40] U. Alon, Nat. Rev. Genet. **8**, 450 (2007).

[41] M. R. Farhat, B. J. Shapiro, K. J. Kieser, R. Sultana *et al.*, Nat. Genet. **45**, 1183 (2013).
[42] M. E. Gorre, M. Mohammed, K. Ellwood, N. Hsu *et al.*, Science **293**, 876 (2001).
[43] C. Roche-Lestienne, J. L. Laï, S. Darré, T. Facon *et al.*, N. Engl. J. Med. **348**, 2265 (2003).
[44] H. Safi, S. Lingaraju, A. Amin, S. Kim *et al.*, Nat. Genet. **45**, 1190 (2013).
[45] H. Zhang, D. Li, L. Zhao, J. Fleming *et al.*, Nat. Genet. **45**, 1255 (2013).
[46] N. Q. Balaban, J. Merrin, R. Chait, L. Kowalik *et al.*, Science **305**, 1622 (2004).
[47] O. Gefen and N. Q. Balaban, FEMS Microbiol. Rev. **33**, 704 (2009).
[48] M. Acar, J. T. Mettetal, and A. van Oudenaarden, Nat. Genet. **40**, 471 (2008).
[49] D. Nevozhay, R. M. Adams, E. V. Itallie, M. R. Bennett *et al.*, PLoS Comput. Biol. **8**, e1002480 (2012).
[50] H. Kobayashi, M. Kaern, M. Araki, K. Chung *et al.*, Proc. Natl. Acad. Sci. USA **101**, 8414 (2004).